Scilight

Materials and Sustainability

https://www.sciltp.com/journals/MatSus

Review

Lead-Free Perovskite and Perovskite-Inspired Materials for Indoor Photovoltaics: A Perspective

EQ Han [1], Jung Ho Yun [1,*] and Miaoqiang Lyu [2,*]

[1] Air & Environment Energy Nexus (A2EN) Lab., Department of Environmental Science and Engineering, College of Engineering, Kyung Hee University, Yongin-si 17104, Gyeonggi-do, Republic of Korea
[2] School of Chemical Engineering, The University of Queensland, St Lucia, QLD 4072, Australia
* Correspondence: jungho.yun@khu.ac.kr (J.H.Y.); m.lyu@uq.edu.au (M.L.)

How To Cite: Han, E.; Yun, J.H.; Lyu, M. Lead-Free Perovskite and Perovskite-Inspired Materials for Indoor Photovoltaics: A Perspective. *Materials and Sustainability* **2026**, *2*(1), 1. https://doi.org/10.53941/matsus.2026.100001

Received: 10 October 2025
Revised: 27 December 2025
Accepted: 7 January 2026
Published: 22 January 2026

Abstract: The past few years have witnessed increasing research interest in lead-free perovskites for indoor photovoltaics. Lead-free perovskites along with many reported perovskite halide analogue compounds take advantage of the solution-processibility, low-toxicity and high-theoretical efficiencies under weak indoor light conditions. Therefore, these semiconductors show promising potential as the next-generation indoor photovoltaics for integration with low-power wearables and internet-of-things electronics. In this perspective, we discuss the overview of the current research progress of lead-free perovskites for IPVs and highlight the challenges in this field as well as the speculative directions for further development.

Keywords: lead-free; perovskite; perovskite-inspired; indoor; photovoltaic; solar cells

1. Introduction

The advent of the Internet of Things (IoT) era has witnessed increasingly widespread adoption of various wearable electronics and wireless sensors, driven by growing consumer demand for healthcare/environmental monitoring, smart homes, building/industrial automation, and data-driven decision making, and so on. The global IoT sensor market alone is predicted to achieve over USD 106 billion by 2030 with a compound annual growth rate (CAGR) of 36.8% from 2024 to 2030 (Grand View Research, Inc., San Francisco, CA, USA) [1]. Most of the IoT sensors operate wirelessly and thus require off-the-grid power sources. Batteries have been predominantly used for powering the IoT sensors, and it is estimated that ~78 million batteries to be replaced daily in 2025, which leads to disruption of device operation, increased maintenance cost and sustainability concerns [2].

In the past decades, indoor photovoltaics (IPVs) have been emerging as a promising alternative solution to address this increasing market demand for low-cost and high-performance off-the-grid power devices. As a large percentage of IoT devices operate in an indoor environment with relatively low power requirements, IPVs can efficiently exploit both ambient and artificial light illumination to enable the IoT operation in battery-free or battery-less modes. For example, ~10 cm^2 mini-module of IPVs with ~30% PCE can achieve a few milliwatts power output under 1000 lux indoor light, which is sufficient for a wide range of indoor IoT gadgets, such as electronic shelf label, asset trackers and building-automation sensors [3]. Different from outdoor sunlight, indoor light features approximately 2–3 orders of magnitude lower irradiation intensity and light spectrum predominantly covering the visible range (400~700 nm, Figure 1a). As a result, solar cells with high efficiencies under the standard sunlight may not perform well under indoor conditions. The optimum bandgap of the light-absorbers for IPVs is 1.8–2.0 eV, so that this can match the indoor light spectra and simultaneously retain a high V_{oc} that is highly desirable for IPVs. Under 1000 lux indoor light illumination using compact fluorescent light (CFL) or light-emitting diodes (LEDs), the theoretical Shockley-Queisser efficiency limit of IPVs can reach 52–57% [4]. Various light-absorbing materials have been studied for IPVs so far, such as amorphous silicon (a-Si), organic polymers, dye sensitizers, $Cu_2ZnSn(S,Se)_4$, GaAs and GaInP [5–9]. Most of this candidates can now delivery over 30%

power conversion efficiency (PCE) under 1000 lux indoor light and the highest reported PCE is 41.4% achieved by the GaInP-based IPVs [6].

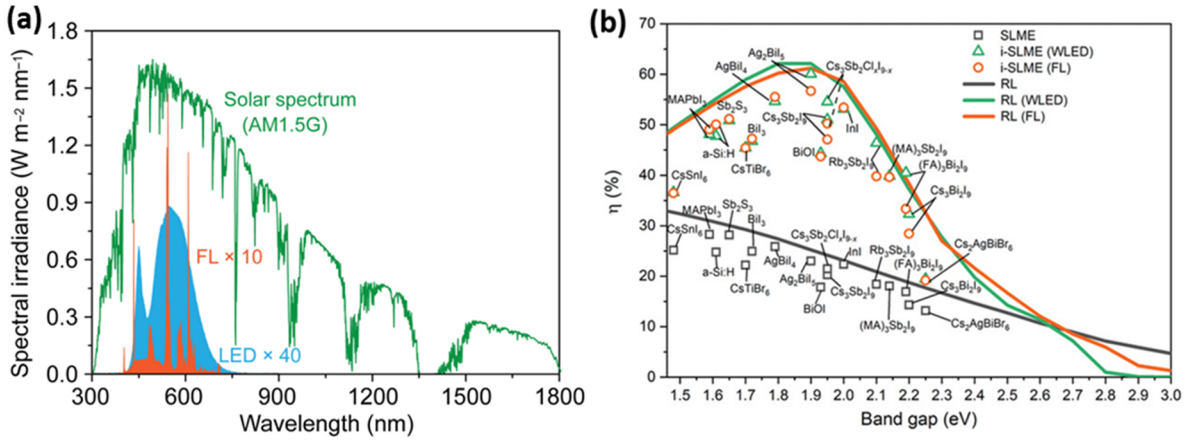

Figure 1. (**a**) Comparison of the standard solar spectrum (AM1.5G) and the typical indoor light spectra. Reproduced with permission from Ref. [10] under a Creative Commons Attribution Non-Commercial License 4.0 (CC-BY). Copyright © 2022 American Association for the Advancement of Science. (**b**) Simulated maximum efficiency of lead-free perovskite and perovskite-inspired materials for IPVs. (SLME: spectroscopically limited maximum efficiency; RL: radiative limit; FL: fluorescent light) Reproduced with permission from Ref. [11] under the terms of the Creative Commons Attribution License. Copyright 2020, Wiley-VCH GmbH.

Recently, metal halide perovskites have been rapidly emerging as the most promising light-absorbing materials for IPVs compared to these existing competing technologies. Despite of comparably short research period, perovskites IPVs have achieved record efficiency around 45% under 1000 lux light illumination, surpassing the other existing IPV technologies [12,13]. This is largely attributed to the advantages of their highly tunable optical bandgaps, intrinsic defect-tolerance, compatibility with solution-based fabrication and low manufacturing cost. According to the calculations based on the indoor spectroscopically limited maximum efficiency (i-SLME) method, the theoretical PCE of halide perovskite IPVs can achieve around 60% given a band gap of ~1.9 eV (Figure 1b) [11]. However, the state-of-the-art metal halide perovskite IPVs employ lead-containing materials (e.g., $Cs_{0.05}FA_{0.70}MA_{0.25}PbI_{2.25}Br_{0.75}$, FA^+: formamidinium and MA^+: methylammonium), and the lead toxicity is prohibited from indoor applications according to the regulations (e.g., the EU Restriction of Hazardous Substances (RoHs) DIRECTIVE 2002/95/EC), which requires <0.1 wt% Pb content in the consumer electronic products [14]. Therefore, lead-free perovskites and perovskite-inspired materials have attracted much attention in IPV studies in the past few years with considerable progress [11,15,16]. An ideal light-absorbing material for IPVs needs to be RoHS-compliant (i.e., low/non-toxicity), stable, efficient and cheap in scale-up manufacturing. In addition, ideal alternatives must also possess outstanding optoelectronic properties, such as a direct band gap for desirable light absorption and photon recycling, defect tolerance for reduced nonradiative recombination, and low and balanced effective masses for facilitated carrier diffusion [17]. While lead-free perovskites represent an extensive family of materials, the current exploration of some typical candidates has shown great promise. This perspective will highlight the achievement obtained to date in developing lead-free perovskites and perovskite-inspired materials for IPVs.

Over the past two decades, many lead-free perovskites and perovskite-inspired materials have been developed and investigated for outdoor solar cells, mainly focusing on tin (Sn), germanium (Ge), bismuth (Bi) and antimony (Sb) based metal halide compounds. Some typical candidates have been reported in IPVs, including tin-based perovskites, and Sb- and Bi-based perovskite analogues in the past few years and the representative IPV efficiencies have been summarized in Table 1. As shown in Figure 2a, the typical tin-based perovskite adopts a structure of $AB(II)X_3$ (A = FA^+, MA^+, Cs^+ or their mixture, B = Sn(II) and X = Br^-, I^- or their mixture). When replacing the metal cations with Bi(III) and Sb(III) at the B site, two typical structures of $A_3B(III)_2X_9$ can be developed with different dimensionality (i.e., a dimer phase with isolated face-sharing octahedra and a layered phase with corner-sharing octahedra). Cation-ordered halide double perovskites (CO-HDPs) with the representative example of $Cs_2AgBiBr_6$ was also studied as another interesting lead-free perovskite candidate. However, "hollow" $AB(II)X_3$ and $A_2B(IV)X_6$ structures have not been reported for IPVs so far. Many of the perovskite-inspired materials exhibit ideal bandgap for IPVs (1.9–2.0 eV). Figure 2b shows several typical

examples of lead-free perovskites and perovskite-inspired materials that have been investigated in IPVs. Their V_{oc} losses are still relatively high, which is one of the limitations for further efficiency improvement. Overall, Sb- and Bi-based perovskite inspired materials show high ambient stability but suffer from relatively low efficiencies under indoor conditions (~10% at 1000 lux) [18]. Sn-based perovskites have been demonstrated promising PCE for IPVs (>21%), but stability is still a big challenge [19].

Table 1. Representative IPV device performance using the typical Sn-based perovskites and Sb-/Bi-based perovskite-inspired materials.

Material	Bandgap/eV	Light Source	Active Area/mm^2	PCE%	V_{oc}/ V	J_{sc}/μA cm^{-2}	FF%	Ref.
$Cs_3Sb_2Cl_xI_{9-x}$ (Dimer)	1.95	WLED, 1000 lux	7.25	4.4	0.47	76	40	[11]
$Cs_3Sb_2Cl_xI_{9-x}$ (Dimer)	1.95	FL, 1000 lux	7.25	4.9	0.49	82	42	[11]
$Cs_{2.4}MA_{0.5}FA_{0.1}Sb_2I_{8.5}Cl_{0.5}$ (Layered)	2.1	WLED, 1000 lux	20	6.37	0.55	102	52	[20]
$MA_{1.5}Cs_{1.5}Sb_2I_3Cl_6$ (Layered)	2.1	WLED, 1250 lux	9	3.0	0.41	42.2	66.6	[21]
$MA_{1.5}Cs_{1.5}Sb_2I_3Cl_6$ (Layered)	2.1	WLED, 1250 lux	252	2.8	1.36	35.8	68.1	[21]
$Cs_2Sb_2I_9$ (Layered)	2.0	WLED 1000 lux	9	8.2%	0.70	102.87	52	[22]
$Cs_2Sb_2I_9$ (Layered)	/	WLED 3000 K, 1000 lux	10	9.2	0.74	47.7	/	[23]
CsMAFA-Sb:Bi	/	WLED, 6500 K, 1000 lux	10	9.6	0.65	73.8	69.3	[18]
Ag_2BiI_5	1.90	WLED 1000 lux	9	5.02	0.70	39.16	48	[24]
$(CH_3NH_3)_3Bi_2I_9$		WLED 1000 lux	/	4.47	NR	NR	NR	[25]
$Cs_2AgBiBr_6$	2.21	WLED 1000 lux	/	7.1	0.85	36.4	76.8	[26]
$Cs_2AgBiBr_6$	2.21	WLED 600 lux	600	7.77	NR	NR	NR	[26]
$ATBiI_4$	/	WLED 4000 K, 1000 lux	2.56	0.52	0.71	4.35	50.55	[27]
$FASnI_2Br$	/	1000 lux	17	11.1	0.58	80	72	[28]
$FA_{0.75}MA_{0.25}SnI_2Br$	/		7.25	12.81	0.28	280	67	[29]
$FA_{0.75}MA_{0.25}SnI_2Br$	1.59	1000 lux	/	17.26	0.55–0.6	/	/	[30]
$FA_{0.75}MA_{0.25}SnBrI_2$	1.63	WLED 1062 lux	7.25	17.57	0.57	162	64	[31]
$FASnI_2Br$	1.63	WLED, 3000K, 1000 lux	9	20.12	0.696	120.5	68.35	[32]
FASnI$_2$Br-4APCl	/	Led 1000 lux	12.25	21.55	0.721	119	72.4	[19]

$ATBiI_4$: ATI = 2-aminothiazolium iodide (ATI).

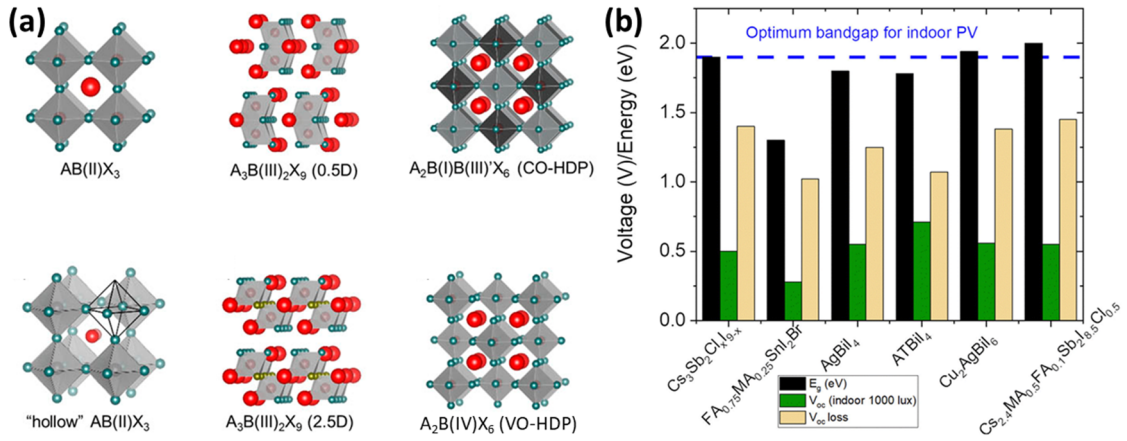

Figure 2. (**a**) Some typical crystal structures of lead-free halide perovskite and perovskite-inspired materials. Reproduced with permission from Ref. [33] under the terms of the Creative Commons CC BY license. Copyright 2020, AIP Publishing LLC. (**b**) Comparison of bandgap, V_{oc} and V_{oc} loss of typical lead-free perovskites and perovskite-inspired materials. Reproduced with permission from Ref. [15] under a Creative Commons Attribution 3.0 Unported Licence. Copyright 2023, Royal Society of Chemistry.

2. Tin-Based Halide Perovskites for IPVs

Among all the available lead-free metal halide perovskite/perovskite analogues, tin-based perovskites are currently the best-performing candidate in high-efficiency lead-free perovskite IPVs. However, the typical Sn^{2+} in the perovskite structure is not stable in ambient atmosphere due to a facile spontaneous oxidation of Sn(II) into Sn(IV). This is primarily originated from the inert-pair expression of the s orbital in Sn, as this is not relatively more stable than its p orbitals [34]. Therefore, a less symmetric distribution of the s orbital electrons presents around the nucleus, leading to serious lattice distortion and enhanced electronic disorders. Owing to this electronic characteristic, some sources of oxidation of tin-based perovskites in solar cells have been identified in addition to the oxygen, such as the precursor solvent (e.g., dimethyl sulfoxide), metal oxide-based electron-transporting layers (e.g., TiO_2 and SnO_2) that have direct contact with the perovskite, and the widely used C_{60} [34]. These can be potentially addressed by isolating the chemical contact with an inert barrier layer or replacing with other non-oxidative alternatives.

In 2021, Catechin was introduced as a dopant in the Sn perovskite precursor to suppress the Sn^{2+} oxidation and tune the interfacial energy levels, leading to around 22% PCE improvement in IPVs [29]. Nicotinamide can modify the work function of the PEDOT:PSS layer, which optimize the energy level alignment for improving Voc of Sn perovskite solar cells from 0.63 V to 0.82 V [30]. In 2022, Cao et al. introduced KSCN interlayer in the $FA_{0.75}MA_{0.25}SnBrI_2$-based perovskite solar cells for optimizing the interfacial energy band alignment, achieving a decent PCE of 17.57% at 1062 lux indoor white light emitting diodes (WLED) [31]. In addition KSCN interfacial layer, CsF was found to be another effective candidate for modifying the buried interface on the PEDOT:PSS layer by reducing the energy barrier for heterogeneous nucleation of Sn perovskite thin film, which can in turn improve the film quality and lead to a PCE of 20.12% for IPVs under 1000 lux [32]. Apart from the interfacial engineering, efforts to enhance Sn perovskite film quality by solvent engineering and additives have witnessed progress. Replacing the typical DMSO with a N,N-diethylformamide and N,N'-dimethylpropyleneurea (DEF:DMPU, 6:1 *v*:*v*) solvent system was demonstrated to be effective in suppressing Sn^{4+} (negligible oxidation from XPS), which in turn leads to 11.1% IPV efficiency under 1000 lux and promising stability performance of up to 6 months without PCE decrease [28]. Very recently, 4-aminopyridine hydrochloride (4APCl) was introduced to control the crystallization of $FASnI_2Br$ perovskite via the formation of the 6H-intermediate phase. By retarding the film growth kinetics, improved film quality was achieved and a PCE of 21.55% at 1000 lux was demonstrated, which is the best reported for Sn perovskite IPVs [19].

Despite only a few handful reports in Sn-based perovskite IPVs, the achieved PCE is the highest among all the existing reports using lead-free perovskite/perovskite-inspired materials, indicating the great promise in high efficiency IPVs. However, the serious stability issue due to the air-sensitivity of Sn(II) is still the main challenge to be addressed. It is worthwhile to conduct systematic stability tests of the Sn-based perovskite IPVs with the state-of-the-art encapsulation, which can provide useful insight for seriously assessing the feasibility of these materials for practical applications. In fact, indoor environment offers ideal setting for Sn-based perovskite devices, where the devices can bypass the serious thermal and UV stability issues, as these materials are known to be less thermally stable compared to their lead counterparts. Unlike lead-based perovskite solar cells, tin-based perovskite solar cell has an ideality factor of approximately 2, indicating significant non-radiative recombination. This also cause considerable drop in V_{oc} when reduce the operational light illumination intensity [35]. The dominant defect species in tin-based perovskites generally originate from the oxidation of Sn^{2+} that leads to deep-level defects. Therefore, developing effective strategies to suppress this non-radiative recombination is critically important for further advancing this technology.

3. Perovskite-Inspired Materials for IPVs

Other lead-free alternatives, such as metal cations with Bi^{3+} and Sb^{3+}, have been studied for IPVs. These two candidates show isoelectronic properties to that of lead and considerably lower toxicity. A high Shockley-Queisser theoretical efficiency up to 62% can be achieved for a bandgap of 1.9 eV under 1000 lux FL and WLED illumination [11]. Indoor spectroscopically limited maximum efficiency (i-SLME) takes account of materials absorption coefficients, thickness and bandgap nature, and thus offers a more realistic estimation of the maximum efficiency, as shown in Figure 1b. The $Cs_3Sb_2Cl_xI_{9-x}$ shows 50–54% i-SLME, which holds great promise for further exploration.

Unlike Sn-based halide perovskites, $Cs_3Sb_2Cl_xI_{9-x}$ shows high material stability under exposure to O_2 and moisture (up to 5 month stability was reported) with even enhanced PCE after long-term stability test [11]. Although the PCE of the IPVs were relatively low (4–5%), the $Cs_3Sb_2Cl_xI_{9-x}$-based IPVs with 7.25 mm^2 device area were demonstrated to be sufficient for operating printed thin-film transistor circuits.[11] A decent V_{oc} of 0.88 V was achieved under 1 sun conditions for $Cs_3Sb_2Cl_xI_{9-x}$-based solar cells [36]. Further improvements was achieved by

developing layered structure instead of the dimer phase in $Cs_{2.4}MA_{0.5}FA_{0.1}Sb_2I_{8.5}Cl_{0.5}$, and an indoor PCE of 6.37% was demonstrated under 1000 lux WLED light.[20] This underscores the importance of the connectivity of Sb-halide octahedra in the device performance, as the layered phase generally exhibits lower effective masses for better charge transport. Very recently, 2D-$Cs_3Sb_2I_9$-based IPVs achieves an i-PCE of 8.2% under WLED 1000 lux light illumination [22]. This exemplifies the importance of dimension of the crystal structure on the device performance. This was realised by retaining the Cl-induced 2D structure, while at the same time suppressing Fröhlich electron–phonon coupling with an anion-exchange strategy, which offers a promising pathway for further improving the device performance for this lead-free candidate. To enhance the light absorption, an indacenodithiophene-based organic acceptor (ITIC), 3,9-bis (2-methylene-(3-(1,1 dicyanomethylene)indanone))-5,5,11,11-tetrakis (4-hexylphenyl)dithieno [2,3-d:2′,3′-d′]-*s*-indaceno[1,2-*b*:5,6-*b*′]dithiophene, was studied as a complementary absorbing ETL. This strategy is effective and enhances the efficiency of $Cs_3Sb_2I_9$-based solar cells, reaching 9.2% under 1000 lux, which is the highest among all the Sb-based reports for IPVs [23].

In 2025, Lamminen and co-workers reported a PCE of 10.11% at 1000 lux using alloyed Sb and Bi-based perovskite-inspired material in a triple A-cation structure [18]. Although a systematic optimisation on the composition of the active layer, interfacial chemistry and device structure was performed to achieve this critical milestone, a thin dimethylphenethylsulfonium iodide (DMPESI)-based surface passivator is one of the key contributor to improve the film microstructure and reduce interfacial photocarrier traps. This represents the best reported IPVs using perovskite-inspired materials. It is worth noting that the stabilised J_{sc} and V_{oc} only achieve 73.8 μA cm^{-2} and 0.65 V, respectively, suggesting significant losses from insufficient light utilisation and non-radiative recombination. Nevertheless, this CsMAFA-Sb:Bi IPV device can deliver a power output density around 31.6 μW cm^{-2} at 1000 lux, which is sufficient to satisfy the demands of several low-power IoTs, such as Bluetooth low energy (BLE) sensors (10–50 μW), electronic shelf labels (5–20 μW), and radio frequency identification (RFID) sensors (10–45 μW).

Other Bi-based perovskite-inspired materials were also investigated with inferior performance. For example, IPVs based on 2-aminothiazolium (AT) bismuth iodide ($ATBiI_4$) was reported with a PCE of 0.52% under the 1000 lux indoor LED [27]. Ag_2BiI_5 IPVs show a PCE of 5.0% under 1000 lux even with a semitransparent film (<100 nm) [24]. A promising V_{oc} up to 0.80 V was also demonstrated for this material. However, serious current-voltage hysteresis was observed. Among the bismuth-based perovskite-inspired materials, $Cs_2AgBiBr_6$ double perovskite have received much attention with a decent PCE of 7.16% at 1000 lux indoor conditions, which is much higher than the other candidates based on bismuth cation only [26]. The first lead-free semitransparent $Cs_2AgBiBr_6$ double perovskite mini modules were also reported, achieving 3.4% indoor efficiency. It's worth noting that the V_{oc} can reach up to 1.293 V, which is desirable for IoT applications with less cells required for module design [37]. Although $Cs_2AgBiBr_6$ double perovskite has a large bandgap of 1.83–2.39 eV, the indirect band characteristic, strong electron-phonon coupling effect and low absorption coefficient (~4×10^4 cm^{-1}) are the limitations for device performance [38,39]. It also suffers from dual-ion diffusion induced material degradation, which, however, might be mitigated under the indoor conditions [38]. Hydrogenated $Cs_2AgBiBr_6$ was demonstrated to be an effective strategy to tune the bandgap (1.64~2.18 eV) and enhance the carrier mobility for outdoor solar cells, achieving a record high efficiency of 6.37% under standard one-sun conditions [40]. Regarding the indoor application, simulations of the IPVs based on hydrogenated $Cs_2AgBiBr_6$ was reported recently with promising PCEs up to 41.03% at 200 lux WLED though, experimental validation of the effectiveness of this hydrogenation strategy for improving its IPV performance still need to be achieved [41]. Another emerging candidate is Cu_2AgBiI_6, which belongs to pnictohalides and adopts a direct bandgap of ~2 eV and high absorption coefficient, and thus holds greater promise than that of the other typical Bi-based halide candidates [42,43]. Alloying Sb(III) into the Cu_2AgBiI_6 crystal was reported to suppress intrinsic defects and carrier self-trapping, and thus significantly improved the photocurrent from 72 μA cm^{-2} up to 128 μA cm^{-2} [42]. A indoor PCE of 9.53% was achieved at 1000 lux, representing the highest reported efficiency for the IPVs using Bi-based pnictohalides.

Preliminary attempts on developing mini-modules have been reported using lead-free perovskite and perovskite-inspired materials [21,44–46]. For example, a flexible mini module of Sn-based perovskite ($(BA_{0.5}PEA_{0.5})_2FA_3Sn_4I_{13}$) IPVs has been demonstrated using a scalable blade-coating method (Figure 3a). This module consists of 8 interconnected cells (25 cm^2 in dimension and 1.5 cm^2 active area for each cell), reaching a decent efficiency of 9.4% under 2000 lux white-LED illumination (Figure 3b) [46]. It`s noted that the laser patterning of the module was conducted in the ambient air, which compromised the device efficiency due to the air exposure and surface oxidation. The addition of an ionic liquid and a reducing $NaBH_4$ in the precursor solution improves the stability of the fabricated Sn perovskites. However, the stability under N_2 atmosphere is still relatively poor, as on 70–80% initial PCE was preserved after 3300h. While air stability of Sn perovskite IPVs is still a significant drawback for module development, mini modules using air stable Sb-based perovskite-inspired

material have been demonstrated recently, achieving a PCE of 2.8% under 1250 lux (Figure 3c) and >80% initial efficiency retention after 1800 h ambient air exposure and h and 60% after 7 months (Figure 3d) [21]. The good air stability of Sb-based perovskite-inspired material is advantageous for scalable fabrication outside the glove box. However, further improvement in PCE is imperative for practical applications.

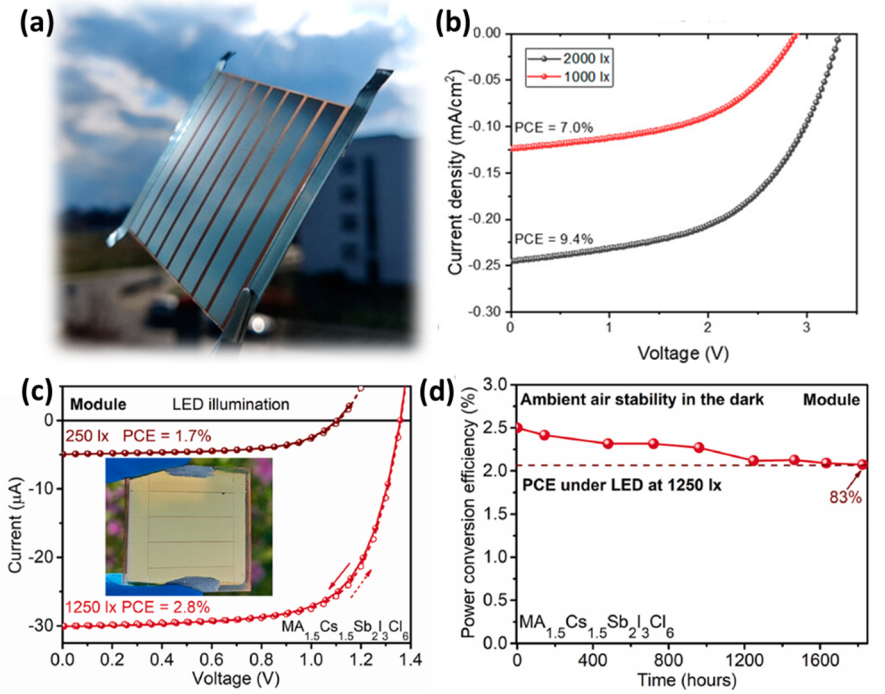

Figure 3. (**a**) Sn-based perovskite IPV module and (**b**) the J-V characteristics of the champion device under 1000 and 2000 lux indoor light; Reproduced with permission from Ref. [46] licensed under CC-BY 4.0. Copyright 2023 American Chemical Society. (**c**) J-V curves of the $MA_{1.5}Cs_{1.5}Sb_2I_3Cl_6$ IPV module and (**d**) long-term stability of the module without encapsulation. Reproduced with permission from Ref. [21] under open access license of Creative Commons CC-BY. Copyright 2025 Elsevier B.V.

4. Challenges and Perspectives

Based on the current progress, there is a compromise between efficiency and stability of lead-free perovskites and perovskite-inspired materials for IPVs applications. While tin-based perovskites have been demonstrated with the best-performing device efficiencies, their ambient stability is still a big challenge. The poor stability of the tin-based perovskite is mainly originated from the oxidation of Sn(II) upon exposure to oxygen or other sources of oxidants during the device fabrication/operation. On the other hand, Sb- or Bi-based perovskite-inspired materials have obvious advantages in ambient stability, the device efficiencies are still only half of that of the Sn-based counterparts in IPVs. The relatively low efficiency is primarily due to several intrinsic properties of these Sb- and Bi-based perovskite-inspired materials, including indirect bandgap, large exciton binding energies (e.g., 175 meV for $Cs_3Sb_2I_9$ [47], vs. 18 meV for $CsSnI_3$ [48]), higher electron and hole effective masses (e.g., $Cs_3Sb_2I_9$: 1.55 and 1.40 for m^*_h and m^*_e [47]; $CsSnI_3$: 0.042 and 0.058 for m^*_h and m^*_e [49]), a strong electron-phono coupling effect, high trap densities (10^{17}~10^{18} cm^{-3}) and serious non-radiative recombination of charge carriers, etc.

To address the stability of Sn-based perovskites, various strategies have been reported for the outdoor applications in the past few years, such as compositional engineering, solvent engineering, additives and passivation of Sn-perovskite bulk/interface [50]. The effectiveness of these strategies can be further investigated for improving the stability under indoor environments. Additionally, defect-induced degradation can be reduced under indoor operation is expected to be minimized for Sn-based perovskites due to the mild conditions (weak light intensity without ultra-violet (UV) component, controlled humidity and temperature). In fact, oxidation of Sn(II) is energetically favored at the top surface and thus passivation of the top interface has been the main focus of the previous research to address both the device efficiency and stability of Sn-based perovskites, which is even more critical in IPVs as the trap-assisted Shockley-Read-Hall recombination become the predominant loss under low-light conditions for IPV operation [13,51]. Currently, the trap-induced non-radiative recombination also leads to the high V_{oc} loss (>0.8 V) in Sn-based perovskite IPVs, indicating significant room for further improvements.

The best-performing Sn-based perovskite IPVs have been using Br-doped Sn perovskites and the bandgap is not optimized (below 1.7 eV) for indoor light spectra. 2D/3D or quasi-2D Sn-based perovskites by tuning the A-site cation offer opportunities for optimum bandgap for IPVs with enhanced material stability, where n-butylamine (BA), phenylethylamine (PEA) and fluorinated PEA cations are some promising options. In addition, device encapsulation is another challenge to be addressed, as this has been rarely explored so far and most of the shelf-life stability and continuous light illumination testing have been conducted on unencapsulated devices in N_2-filled glove boxes. While the stability is the main obstacle for Sn-based perovskites, efficiencies of the IPVs are anticipated to be further improved by reducing V_{oc} loss caused by the defect-induced non-radiative recombination and optimizing the bandgap for a better spectrum match. It is encouraging that precursor additives such as ionic liquid and reducing agent (e.g., $NaBH_4$) can enable ambient process for laser patterning of the Sn-based perovskite IPVs. More systematic screening and studies to identify other additives represents a promising pathway towards practical applications of the Sn-based perovskite IPVs.

In terms of the lead-free Sb- and Bi-based perovskite-inspired materials, the intrinsic properties are main limitations of their inferior efficiency in IPVs. While the higher valence of the Sb and Bi metal cations leads to much stronger metal-halide bonds that enhances the structural stability of the metal octahedra compared to that of the Pb and Sn-based perovskites, their smaller ionic radii facilitate the formation of low-dimensional structures instead of typical 3D perovskites. The reduced structural dimension is not preferred for efficient charge transport. In addition, the indirect bandgap for most of the existing Sb- and Bi-based perovskite-inspired materials is unfavorable for IPVs due to less efficient photon absorption due to phonon-assisted process, which also creates additional pathways for non-radiative recombination. These materials also generally show larger effective masses for electrons and hoes, which is undesirable for efficient photo-generated charge transport. However, some effective strategies have been proven to significantly boost the device performance and offer useful implications for further research and development in this direction. Unlike the tin-based perovskites that show excellent light-absorption capabilities, most of the Sb- and Bi-based candidates have indirect optical bandgap. Searching for direct bandgap candidates with better light-absorption properties has led to the discovery of some promising pnictohalides (e.g., Cu_2AgBiI_6). Considering the combinatorial chemistry of available lead-free perovskites and their derivatives, immense opportunities are still to be explored to evaluate the material properties and their suitability for IPV applications. To this end, ab initio simulations combined with machine learning can be a powerful tool set for fast screening for better candidate materials. To further improve the IPV efficiency that is limited by the relatively strong exciton-phonon coupling in many of these materials, composition engineering (e.g., alloying Sb cations) has been effective for modulating the local symmetry of the crystal polyhera, which can reduce the self-trapping induced charge carrier localization [52]. Similar to the Sn-based perovskites, high-quality thin-films are the prerequisites for high-performance devices. Therefore, film processing for optimum morphology and defect passivation are key to minimize trap-assisted Shockley-Read-Hall recombination of the photogenerated charge carriers at the interfaces and grain boundaries under the weak light.

Simulations of various types of lead-free perovskites have been conducted to assess the suitability of these materials for IPVs, including Ge-Sn mixed perovskites [53], $AgBiI_4$ [54], Cs_2SnI_6 [55], and hydrogenated $Cs_2AgBiBr_6$ [41]. In particular, hydrogenated $Cs_2AgBiBr_6$ can achieve a reduced optical bandgap of 1.97 eV, which is attractive for IPVs with better spectral matches. Promising results were achieved from the simulations though, experimental verification is relatively lagging behind and should be performed to confirm their real potential. In addition, lead-free quaternary mixed-metal chalcohalides may offer extensive opportunities owing to suitable direct bandgaps, which have been rarely explored for IPVs [56]. Lead-free chalcogen perovskites, such as $CaZrS_3$, $SrZrS_3$ and $BaZrS_3$, have recently attracted attention due to their superior optoelectronic properties, including ideal bandgaps, high light absorption coefficient and low deep-level defects [57]. These emerging lead-free perovskite alternatives may have the potential to overcome the current stability and efficiency challenges in the existing candidates, but this requires future efforts to experimentally validate their potential. In addition, the development of high-performance lead-free wide-bandgap light-absorbers may benefit their potential applications in tandem cells for outdoor PVs as the top cells.

Indoor environment offers very mild operation conditions compared to that of the standard one-sun, including 2–3 orders of magnitude lower light intensity, no ultra-violet light, relatively stable and controlled humidity levels and negligible light-illumination induced temperature variations. Therefore, IPVs based on lead-free perovskites and perovskite-inspired materials are expected to suffer from less challenging operational stability issues compared to the outdoor applications. In fact, many start-up companies commercializing perovskite solar cells have also envisioned IPVs for consumer electronics as the most feasible and competitive product on the market, including Saule Technologies (Poland), Halocell (Australia), Mellow Energy (China), Perovskia (Switzerland), Solaries Entreprises (Canada), Xi`an Tianjiao New Energy (China) and FAB Solar (China), etc. Some of these companies

have already provided products of IPV integrated IoT devices to the market, even though all these IPVs are still using lead-based perovskites. Currently, long-term operational stability results of IPVs, regardless of lead or lead-free perovskites, are still quite limited. A standard assessment procedure for long-term/accelerated operational stability testing under indoor light conditions should be developed. For IPVs based on lead-free perovskites and perovskite-inspired materials, the stability data of encapsulated devices is particularly important to evaluate the operational stability that can be enabled by the state-of-the-art encapsulation technology, as the tin-based perovskites would be highly relying on the rigid physical barriers to prevent oxidation in ambient conditions.

In addition, it is imperative to test the IPV devices with standard efficiency evaluation procedure, which can allow comparable performance from different research groups. Although the International Electrotechnical Commission (IEC) has developed a relevant standard for IPVs, detailed description of the testing protocols is still missing. In fact, indoor light sources, such as WLED and FL, have temporal instability and spatial non-uniformity, which is the main source of inaccuracies of the IPV characterizations. To benchmark the testing for meaningful comparisons among different research groups, a combined testing method should be adopted, including spectral irradiance calibration by an authorized institution, report of total irradiance of illumination conditions, and using standard reference irradiances, and eliminate angular issues among the light source and testing devices [58]. National Institute of Standards and Technology (NIST) actually introduced reference irradiance spectra (CCT3000K, CCT4000K and CCT6000K), which can be a good reference for IPV performance test and report for interlaboratory comparisons.

Although the existing lead-free cations (e.g., Sn(II), Bi(III) and Sb(III)) are considered as lower toxicity alternatives to lead, it is worth noting that relevant research on the toxicity assessment of these lead-free perovskites/perovskite-inspired materials is well under-explored to date, and thus argument still remains under debate regarding their feasibility as practical low-toxicity replacement [59–62]. For example, while Bi-based perovskite-inspired materials have been investigated for IPVs as low-toxicity candidates [63,64], a very recent cytotoxicity study raises the concern that Bi compounds show a similar toxicity profile to Pb perovskites with potential pulmonary-hepato-hemotoxicity [59]. Nevertheless, the life-cycle-assessment of the Sb- and Bi-based halide compounds supports the claim of these materials may potentially show reduced environmental burden over the typical a-Si:H for IPVs. Sn-based perovskites exhibit Instead of assessing the toxicity of the metal cations, the toxicity assessment should also consider the material stability, life cycle impacts, recycling, formulations and concentrations. More systematic research is still needed to resolve the existing debates and investigate the cytotoxicity of these lead-free alternatives.

Overall, despite increasing attention in recent years, research into IPVs based on lead-free perovskite/perovskite-inspired materials is still at very early research stage with many unanswered questions and critical challenges to be addressed. Further improvements in the stability of lead-free perovskites or the efficiency of perovskite-inspired materials represent the future milestones towards low-toxicity and high-performance IPVs for practical applications.

Author Contributions

E.H.: Writing—review & editing, Writing—original draft, Methodology, Formal analysis, Data curation. J.H.Y.: Writing—review & editing, Supervision, Funding acquisition, Conceptualization. M.L.: Writing—review & editing, Supervision, Conceptualization. All authors have read and agreed to the published version of the manuscript.

Funding

This work was supported by the Global STEM Professorship Scheme of the Hong Kong government, a National Research Foundation (NRF) of Korea grant funded by the Korean government (MEST) (RS-2023-00257494 and RS-2024-00333809). M.L. acknowledges the financial support from the Australian Research Council (ARC) through Discovery Early Career Researcher Award (DECRA) Fellowship and Discovery project, and Advance Queensland Industry Fellowships from Queensland Government.

Institutional Review Board Statement

Not applicable.

Informed Consent Statement

Not applicable.

Data Availability Statement

The data that support the findings of this study are available from the corresponding author upon reasonable request.

Conflicts of Interest

The authors declare no conflict of interest.

Use of AI and AI-Assisted Technologies

There is no AI or AI-assisted technology used in this article.

References

1. Grand View Research, Inc. Available online: https://www.grandviewresearch.com/industry-analysis/iot-sensors-market-report (accessed on 21 August 2025).
2. EnABLES—European Infrastructure Powering the Internet of Things. EnABLES Position Paper Coordinated by Tyndall Recommends Key Actions to Power IoT in a Reliable and Sustainable Way. EnABLES—European Infrastructure Powering the Internet of Things. EnABLES Position Paper Coordinated by Tyndall Recommends Key Actions to Power IoT in a Reliable and Sustainable Way. EnABLES. Available online: https://www.enables-project.eu/outputs/position-paper/ (accessed on 26 August 2025).
3. Grandhi, G.K.; Koutsourakis, G.; Blakesley, J.C.; et al. Promises and challenges of indoor photovoltaics. *Nat. Rev. Clean Technol.* **2025**, *1*, 132–147. https://doi.org/10.1038/s44359-024-00013-1.
4. Ho, J.K.W.; Yin, H.; So, S.K. From 33% to 57%–an elevated potential of efficiency limit for indoor photovoltaics. *J. Mater. Chem. A* **2020**, *8*, 1717–1723. https://doi.org/10.1039/C9TA11894B.
5. Kim, G.; Lim, J.W.; Kim, J.; et al. Transparent thin-film silicon solar cells for indoor light harvesting with conversion efficiencies of 36% without photodegradation. *ACS Appl. Mater. Interfaces* **2020**, *12*, 27122–27130. https://doi.org/10.1021/acsami.0c04517.
6. Klitzke, M.; Schygulla, P.; Klein, C.; et al. Optimization of GaInP absorber design for indoor photovoltaic conversion efficiency above 40%. *Appl. Phys. Lett.* **2025**, *127*. https://doi.org/10.1063/5.0277001.
7. Zhang, T.; An, C.; Xu, Y.; et al. A Medium-Bandgap Nonfullerene Acceptor Enabling Organic Photovoltaic Cells with 30% Efficiency under Indoor Artificial Light. *Adv. Mater.* **2022**, *34*, e2207009. https://doi.org/10.1002/adma.202207009.
8. Jebin, P.R.; George, A.S.; Mishra, R.K.; et al. Enhanced indoor photovoltaic efficiency of 40% in dye-sensitized solar cells using cocktail starburst triphenylamine dyes and dual-species copper electrolyte. *J. Mater. Chem. A* **2024**, *12*, 32721–32734. https://doi.org/10.1039/D4TA05513F.
9. Deng, H.; Sun, Q.; Yang, Z.; et al. Novel symmetrical bifacial flexible CZTSSe thin film solar cells for indoor photovoltaic applications. *Nat. Commun.* **2021**, *12*, 3107. https://doi.org/10.1038/s41467-021-23343-1.
10. Mathews, I.; Kantareddy, S.N.; Buonassisi, T.; et al. Technology and market perspective for indoor photovoltaic cells. *Joule* **2019**, *3*, 1415–1426. https://doi.org/10.1016/j.joule.2019.03.026.
11. Peng, Y.; Huq, T.N.; Mei, J.; et al. Lead-Free Perovskite-Inspired Absorbers for Indoor Photovoltaics. *Adv. Energy Mater.* **2020**, *11*, 2002761. https://doi.org/10.1002/aenm.202002761.
12. Ma, Q.; Wang, Y.; Liu, L.; et al. One-step dual-additive passivated wide-bandgap perovskites to realize 44.72%-efficient indoor photovoltaics. *Energy Environ. Sci.* **2024**, *17*, 1637–1644. https://doi.org/10.1039/d3ee04022d.
13. Wang, Y.; Yang, T.; Cai, W.; et al. Defect Passivation Refinement in Perovskite Photovoltaics: Achieving Efficiency over 45% under Low-Light and Low-Temperature Dual Extreme Conditions. *Adv. Mater.* **2024**, *36*, e2312014. https://doi.org/10.1002/adma.202312014.
14. Moody, N.; Sesena, S.; deQuilettes, D.W.; et al. Assessing the regulatory requirements of lead-based perovskite photovoltaics. *Joule* **2020**, *4*, 970–974. https://doi.org/10.1016/j.joule.2020.03.018.
15. Grandhi, G.K.; Jagadamma, L.K.; Sugathan, V.; et al. Lead-free perovskite-inspired semiconductors for indoor light-harvesting - the present and the future. *Chem. Commun.* **2023**, *59*, 8616–8625. https://doi.org/10.1039/d3cc01881d.
16. Polyzoidis, C.; Rogdakis, K.; Kymakis, E. Indoor Perovskite Photovoltaics for the Internet of Things—Challenges and Opportunities toward Market Uptake. *Adv. Energy Mater.* **2021**, *11*. https://doi.org/10.1002/aenm.202101854.

17. Giustino, F.; Snaith, H.J. Toward Lead-Free Perovskite Solar Cells. *ACS Energy Lett.* **2016**, *1*, 1233–1240. https://doi.org/10.1021/acsenergylett.6b00499.
18. Lamminen, N.; Lahtinen, J.; Krishnaiah, M.; et al. Surpassing the 10% Efficiency Threshold in Perovskite-Inspired Indoor Photovoltaics. *ACS Energy Lett.* **2025**, *10*, 3415–3418. https://doi.org/10.1021/acsenergylett.5c01472.
19. Abdel-Shakour, M.; Wang, J.; Huang, J.; et al. 6H-Intermediate Phase Enabled Slow Crystal Growth of Tin Halide Perovskites for Indoor Photovoltaics. *Angew. Chem. Int. Ed.* **2025**, *64*, e202421547. https://doi.org/10.1002/anie.202421547.
20. Lamminen, N.; Grandhi, G.K.; Fasulo, F.; et al. Triple A-Site Cation Mixing in 2D Perovskite-Inspired Antimony Halide Absorbers for Efficient Indoor Photovoltaics. *Adv. Energy Mater.* **2022**, *13*, 2203175. https://doi.org/10.1002/aenm.202203175.
21. Xu, J.; Castriotta, L.A.; Skafi, Z.; et al. Lead-free solar cells and modules with antimony-based perovskite inspired materials for indoor photovoltaics. *Mater. Today Energy* **2025**, *49*, 101823. https://doi.org/10.1016/j.mtener.2025.101823.
22. Guo, Y.X.; Zhao, F.; Zhang, C.J.; et al. Suppressing the Electron-Phonon Coupling in 2D Perovskite $Cs_3Sb_2I_9$ for Lead-Free Indoor Photovoltaics. *Adv. Sci.* **2025**, *12*, e09281. https://doi.org/10.1002/advs.202509281.
23. Singh, A.; Lai, P.T.; Mohapatra, A.; et al. Panchromatic heterojunction solar cells for Pb-free all-inorganic antimony based perovskite. *Chem. Eng. J.* **2021**, *419*, 129424. https://doi.org/10.1016/j.cej.2021.129424.
24. Guerrero, N.B.C.; Guo, Z.L.; Shibayama, N.; et al. A Semitransparent Silver-Bismuth Iodide Solar Cell with V_{oc} above 0.8 V for Indoor Photovoltaics. *ACS Appl. Energ. Mater.* **2023**, *6*, 10274–10284. https://doi.org/10.1021/acsaem.3c00223.
25. Kumar, R.; Liu, H.R.; Nabavi, S.A.; et al. Impact of Indium Doping in Lead-Free $(CH_3NH_3)_3Bi_{2-x}In_xI_9$ Perovskite Photovoltaics for Indoor and Outdoor Light Harvesting. *ACS Appl. Electron. Mater.* **2024**, *6*, 8360–8368. https://doi.org/10.1021/acsaelm.4c01576.
26. Barichello, J.; Shankar, G.; Mariani, P.; et al. Unveiling the potential of $Cs_2AgBiBr_6$ perovskites for next-generation see-through photovoltaics. *Mater. Today Energy* **2024**, *46*, 9. https://doi.org/10.1016/j.mtener.2024.101725.
27. Arivazhagan, V.; Gun, F.; Reddy, R.K.K.; et al. Indoor light harvesting lead-free 2-aminothiazolium bismuth iodide solar cells. *Sustain. Energ. Fuels* **2022**, *6*, 3179–3186. https://doi.org/10.1039/d1se02017j.
28. Panda, D.P.; Issaoui, R.; Iqbal, Z.; et al. DMSO-Free Tin Halide Perovskites for Indoor Photovoltaics. *Acs Energy Lett.* **2025**, *10*, 3789–3798. https://doi.org/10.1021/acsenergylett.5c01581.
29. Yang, W.F.; Cao, J.J.; Dong, C.; et al. Suppressed oxidation of tin perovskite by Catechin for eco-friendly indoor photovoltaics. *Appl. Phys. Lett.* **2021**, *118*, 6. https://doi.org/10.1063/5.0032951.
30. Yang, W.F.; Cao, J.J.; Chen, J.; et al. Nicotinamide-Modified PEDOT:PSS for High Performance Indoor and Outdoor Tin Perovskite Photovoltaics. *Sol. RRL* **2021**, *5*, 7. https://doi.org/10.1002/solr.202100713.
31. Cao, J.-J.; Lou, Y.-H.; Yang, W.-F.; et al. Multifunctional potassium thiocyanate interlayer for eco-friendly tin perovskite indoor and outdoor photovoltaics. *Chem. Eng. J.* **2022**, *433*, 133832. https://doi.org/10.1016/j.cej.2021.133832.
32. Gao, Z.; Wang, J.F.; Xiao, H.B.; et al. Adhesion-Controlled Heterogeneous Nucleation of Tin Halide Perovskites for Eco-Friendly Indoor Photovoltaics. *Adv. Mater.* **2024**, *36*, 2403413. https://doi.org/10.1002/adma.202403413.
33. Pecunia, V.; Occhipinti, L.G.; Chakraborty, A.; et al. Lead-free halide perovskite photovoltaics: Challenges, open questions, and opportunities. *APL Mater.* **2020**, *8*, 12. https://doi.org/10.1063/5.0022271.
34. Abate, A. Stable Tin-Based Perovskite Solar Cells. *ACS Energy Lett.* **2023**, *8*, 1896–1899. https://doi.org/10.1021/acsenergylett.3c00282.
35. Luo, X.H.; Liu, X.; Han, L.Y. Lead-free perovskite solar cells, what's next? *Next Energy* **2023**, *1*, 3. https://doi.org/10.1016/j.nxener.2023.100011.
36. Guo, Y.X.; Zhou, J.; Zhao, F.; et al. Carbon-based 2D-layered $Rb_{0.15}Cs_{2.85}Sb_2Cl_xI_{9-x}$ solar cells with superior open-voltage up to 0.88 V. *Nano Energy* **2021**, *88*, 106281. https://doi.org/10.1016/j.nanoen.2021.106281.
37. Schmitz, F.; Lago, N.; Fagiolari, L.; et al. High Open-Circuit Voltage $Cs_2AgBiBr_6$ Carbon-Based Perovskite Solar Cells via Green Processing of Ultrasonic Spray-Coated Carbon Electrodes from Waste Tire Sources. *ChemSusChem* **2022**, *15*, 10. https://doi.org/10.1002/cssc.202201590.
38. Ghasemi, M.; Zhang, L.; Yun, J.H.; et al. Dual-ion-diffusion induced degradation in lead-free $Cs_2AgBiBr_6$ double perovskite solar cells. *Adv. Funct. Mater.* **2020**, *30*, 2002342. https://doi.org/10.1002/adfm.202002342.
39. Huang, J.; Xiang, H.; Ran, R.; et al. Fundamental understanding in the performance-limiting factors of $Cs_2AgBiBr_6$-based perovskite photovoltaics. *Renew. Sustain. Energy Rev.* **2024**, *191*, 114187. https://doi.org/10.1016/j.rser.2023.114187.
40. Zhang, Z.; Sun, Q.; Lu, Y.; et al. Hydrogenated $Cs_2AgBiBr_6$ for significantly improved efficiency of lead-free inorganic double perovskite solar cell. *Nat. Commun.* **2022**, *13*, 3397. https://doi.org/10.1038/s41467-022-31016-w.
41. Alanazi, T.I.; Shaker, A.; Selim, D. Performance analysis of hydrogenated $Cs_2AgBiBr_6$ perovskite solar cells under white LED illumination. *J. Alloy. Compd.* **2025**, *1010*, 177354. https://doi.org/10.1016/j.jallcom.2024.177354.
42. Al-Anesi, B.; Grandhi, G.K.; Pecoraro, A.; et al. Antimony-bismuth alloying: the key to a major boost in the efficiency of lead-free perovskite-inspired indoor photovoltaics. *ChemRxiv* **2023**. https://doi.org/10.26434/chemrxiv-2023-nb5jj.
43. Grandhi, G.K.; Al-Anesi, B.; Pasanen, H.; et al. Enhancing the Microstructure of Perovskite-Inspired Cu-Ag-Bi-I Absorber for Efficient Indoor Photovoltaics. *Small* **2022**, *18*, e2203768. https://doi.org/10.1002/smll.202203768.

44. Li, X.; Nasti, G.; Dreessen, C.; et al. Printing of tin perovskite solar cells via controlled crystallization. *Sustain. Energ. Fuels* **2025**, *9*, 2063–2071. https://doi.org/10.1039/d4se01321b.
45. Uppara, B.; Singh, S.; Avasthi, S.; et al. Optimization of laser patterning process for eco-friendly tin-halide perovskite solar module–with a nanosecond green laser. *Thin Solid Film.* **2024**, *807*, 140542. https://doi.org/10.1016/j.tsf.2024.140542.
46. Zuraw, W.; Vinocour Pacheco, F.A.; Sanchez-Diaz, J.; et al. Large-Area, Flexible, Lead-Free Sn-Perovskite Solar Modules. *ACS Energy Lett.* **2023**, *8*, 4885–4887. https://doi.org/10.1021/acsenergylett.3c02066.
47. Correa-Baena, J.-P.; Nienhaus, L.; Kurchin, R.C.; et al. A-site cation in inorganic $A_3Sb_2I_9$ perovskite influences structural dimensionality, exciton binding energy, and solar cell performance. *Chem. Mater.* **2018**, *30*, 3734–3742. https://doi.org/10.1021/acs.chemmater.8b00676.
48. Chen, Z.; Yu, C.; Shum, K.; et al. Photoluminescence study of polycrystalline $CsSnI_3$ thin films: Determination of exciton binding energy. *J. Lumin.* **2012**, *132*, 345–349. https://doi.org/10.1016/j.jlumin.2011.09.006.
49. Wuttig, M.; Schön, C.F.; Schumacher, M.; et al. Halide perovskites: Advanced photovoltaic materials empowered by a unique bonding mechanism. *Adv. Funct. Mater.* **2022**, *32*, 2110166. https://doi.org/10.1002/adfm.202110166
50. Zhang, Z.; Huang, Y.; Jin, J.; et al. Mechanistic understanding of oxidation of tin-based perovskite solar cells and mitigation strategies. *Angew. Chem. Int. Ed.* **2023**, *62*, e202308093. https://doi.org/10.1002/anie.202308093.
51. Ricciarelli, D.; Meggiolaro, D.; Ambrosio, F.; et al. Instability of tin iodide perovskites: bulk p-doping versus surface tin oxidation. *ACS Energy Lett.* **2020**, *5*, 2787–2795. https://doi.org/10.1021/acsenergylett.0c01174.
52. Vidal, R.; Lamminen, N.; Holappa, V.; et al. Assessing the Environmental Impact of Pnictogen-based Perovskite-Inspired Materials for Indoor Photovoltaics. *Adv. Energy Mater.* **2025**, *15*, 16. https://doi.org/10.1002/aenm.202403981.
53. Srinu, D.; Kumar, A. Lead-free, stable, mixed SnGe perovskites for light to electricity conversion applications in indoor and space conditions. *J. Comput. Electron.* **2025**, *24*, 13. https://doi.org/10.1007/s10825-025-02367-6.
54. Salem, M.S.; Shaker, A.; Salah, M.M.; et al. Comprehensive TCAD simulation and optimization of lead-free $AgBiI_4$ solar cells: Migration from single cell to high-performance indoor photovoltaic modules. *Ain Shams Eng. J.* **2025**, *16*, 17. https://doi.org/10.1016/j.asej.2025.103371.
55. Arif, M.Z.; Zhou, G.B.; Hasan, M.M. ANN-integrated modeling of HTL-free Cs_2SnI_6 perovskite solar cells under indoor and outdoor light spectra. *J. Alloy. Compd.* **2025**, *1036*, 21. https://doi.org/10.1016/j.jallcom.2025.181801.
56. Henkel, P.; Li, J.R.; Grandhi, G.K.; et al. Screening Mixed-Metal $Sn_2M(III)Ch_2X_3$ Chalcohalides for Photovoltaic Applications. *Chem. Mater.* **2023**, *35*, 7761–7769. https://doi.org/10.1021/acs.chemmater.3c01629.
57. Njema, G.G.; Kibet, J.K. A review of chalcogenide-based perovskites as the next novel materials: Solar cell and optoelectronic applications, catalysis and future perspectives. *Next Nanotechnol.* **2025**, *7*, 100102. https://doi.org/10.1016/j.nxnano.2024.100102.
58. Jailani, J.M.; Luu, A.; Salvosa, E.; et al. Accurate Performance Characterization, Reporting, and Benchmarking for Indoor Photovoltaics. *Joule* **2024**, *9*, 102126. https://doi.org/10.1016/j.joule.2025.102126.
59. Maietta, I.; Otero-Martínez, C.; Fernández, S.; et al. The toxicity of lead and lead-free perovskite precursors and nanocrystals to human cells and aquatic organisms. *Adv. Sci.* **2025**, *12*, 2415574. https://doi.org/10.1002/advs.202415574.
60. Li, J.; Cao, H.-L.; Jiao, W.-B.; et al. Biological impact of lead from halide perovskites reveals the risk of introducing a safe threshold. *Nat. Commun.* **2020**, *11*, 310. https://doi.org/10.1038/s41467-019-13910-y.
61. Schileo, G.; Grancini, G. Lead or no lead? Availability, toxicity, sustainability and environmental impact of lead-free perovskite solar cells. *J. Mater. Chem. C* **2021**, *9*, 67–76. https://doi.org/10.1039/D0TC04552G.
62. Ma, X.; Yao, X.; Zhao, Y.; et al. Life cycle toxicity and reduction potential analysis of perovskite photovoltaic technology. *J. Environ. Manag.* **2025**, *393*, 127170. https://doi.org/10.1016/j.jenvman.2025.127170.
63. Grandhi, G.K.; Toikkonen, S.; Al-Anesi, B.; et al. Perovskite-inspired Cu_2AgBiI_6 for mesoscopic indoor photovoltaics under realistic low-light intensity conditions. *Sustain. Energ. Fuels* **2023**, *7*, 66–73. https://doi.org/10.1039/d2se00995a.
64. Krishnaiah, M.; Singh, K.; Monga, S.; et al. Perovskite-Inspired $Cs_2AgBi_2I_9$: A Promising Photovoltaic Absorber for Diverse Indoor Environments. *Adv. Energy Mater.* **2024**, *15*, 2404547. https://doi.org/10.1002/aenm.202404547.